Mon. Not. R. Astron. Soc. **000**, 1–8 (2014) Printed 8 December 2014 (MN LATEX style file v2.2)

Polar-ring galaxies: the SDSS view on the symbiotic galaxies

V. Reshetnikov[1], F. Combes[2]
[1] *St.Petersburg State University, Universitetskij pr. 28, 198504 St.Petersburg, Stary Peterhof, Russia*
[2] *LERMA, Observatoire de Paris, CNRS (UMR 8112), 61, Av. de l'Observatoire, F-75014 Paris, France*

arXiv:1412.2016v1 [astro-ph.GA] 5 Dec 2014

Accepted 2014 December 5. Received 2014 November 23; in original form 2014 October 1

ABSTRACT

Polar-ring galaxies are multi-spin systems, showing star formation in a blue late-type component, perpendicular to a red early-type one, revealing how galaxy formation can sometimes occur in successive steps. We perform two-dimensional decomposition in the g, r, i bandpasses of 50 polar-ring galaxies (PRGs) from the Sloan Digital Sky Survey. Each object was fit with a Sérsic host galaxy and a Sérsic ring. Our general results are: (i) The central (host) galaxies of the PRGs are non-dwarf sub-L^* galaxies with colors typical for early-type galaxies. (ii) Polar structures in our sample are, on average, fainter and bluer than their host galaxies. (iii) In most galaxies, the stellar mass M_* of the polar component is not negligible in comparison with that of the host. (iv) The distributions of the host galaxies on the size – luminosity and Kormendy diagrams are shifted by $\sim 1^m$ to fainter magnitudes in comparison with E/S0 galaxies. It means that the PRGs hosts are more similar to quenched disks than to ordinary early-type galaxies. (v) All the PRGs in our sample are detected in mid-infrared by WISE, and we derive from the 22μm luminosity their star formation rate (SFR). Their SFR/M_* ratio is larger than for the early-type galaxy sample of Atlas^{3D}, showing that the star forming disk brings a significant contribution to the new stars. Globally, PRGs appear frequently on the green valley in the mass-color diagram, revealing the symbiotic character between a red-sequence host and a blue cloud ring.

Key words: galaxies: statistics – galaxies: structure.

1 INTRODUCTION

Polar-ring galaxies (PRGs) are peculiar galaxies, consisting of a ring or disc of gas, stars and dust orbiting in a plane nearly perpendicular to the major axis of a central galaxy (Whitmore et al. 1990 = PRC). The central object is usually an early-type galaxy (ETG), poor in gas. The polar ring is generally younger and looks similar to late-type galaxies, with large amount of HI gas and young stars. PRGs are very rare objects – the observed fraction of PRGs has been estimated to ∼0.5% of all S0 galaxies (Whitmore et al. 1990; Reshetnikov et al. 2011).

To explain the structure of PRGs, several scenarios have been proposed: (1) the accretion scenario, where two interacting galaxies exchange mass (Reshetnikov & Sotnikova 1997); (2) the merging scenario (Bekki 1997, 1998; Bournaud & Combes 2003); (3) the cosmic formation scenario, where the PRG form through the misaligned accretion of gas from cosmic filaments (Maccio et al. 2006; Brook et al. 2008).

PRGs are important laboratories to study the shape of their dark matter haloes (e.g. Combes 2014), and gain insight into the galaxy formation through late infall, because of the high inclination of their off-plane structures and the evidence of very recent or occuring gas infall.

In summary, galaxies with polar rings are a unique class of extragalactic objects allowing to investigate a wide range of problems, linked with the formation and evolution of galaxies, and to study the properties of their dark haloes. The progress in the study of PRGs is strongly constrained by a small number of known objects of this type. In order to resolve this situation, a new catalogue of PRGs, supplementing the catalogue of Whitmore et al. (1990), have been created (Moiseev et al. 2011 = SPRC). This catalogue consists of 275 candidates to polar-rings galaxies selected from the images of the Sloan Digital Sky Survey (SDSS DR7). The new catalogue significantly increases the number of genuine PRG candidates, and may serve as a good basis both for the further detailed study of individual galaxies, and for the statistical analysis of PRGs as a separate class of objects.

© 2014 RAS

The main purpose of this paper is to study the general photometric characteristics of PRGs from the Sloan Survey. Throughout this article, we adopt a standard flat ΛCDM cosmology with Ω_m=0.3, Ω_Λ=0.7, H_0=70 km s^{-1} Mpc^{-1}.

2 THE SAMPLE AND THE DECOMPOSITION TECHNIQUES

Our sample uncludes 46 objects from the "best candidates" of the SPRC. This group consists of 70 galaxies which are morphologically similar to well-studied "classic" PRGs from Whitmore et al. catalogue. These galaxies tend to have symmetrical central body, resembling early-type galaxies (E/S0), and extended, mostly visible "edge-on" structures crossing the central galaxy at large angles. At the intersections of polar structures and host galaxies are sometimes visible absorption band. Initial analysis of the sample showed that at least two galaxies (SPRC-22 and SPRC-43) are line-of-sight projections of two galaxies, and these objects were excluded from further consideration. From the sample were excluded also too weak and small by angular size objects and also galaxies, showing strongly asymmetric polar structures. The final sample was supplemented with 4 kinematically-confirmed PRGs from Whitmore et al. (1990) catalogue. The list of the sample galaxies is presented in the Table 1, where we provide the basic information about them. Currently, 12 of 50 galaxies in the sample are kinematically-confirmed PRGs (8 from the SPRC – see Moiseev et al. 2014 and 4 from the PRC).

The 2D decomposition of the galaxy images from the sample of 50 PRGs was performed using the GALFIT code (v3.0.4; Peng et al. 2010). GALFIT allows for various parametric functions (Sérsic, Gaussian, etc.) to be modelled simultaneously as either multiple subcomponents of a single object, multiple objects in a frame or combination thereof.

Galaxy images in the g, r and i bands were downloaded from the SDSS DR9 (Ahn et al. 2012). All stars, background and underground objects were masked. Nearby unsaturated stars were used as estimates of the PSF at the objects positions. We fit a two-component model (host galaxy + ring) to all galaxies in the sample. Both components were fitted by a single Sérsic function with seven free parameters (object centres, total magnitude, effective radius r_e, Sérsic index n, ellipticity, position angle). In several cases (e.g. SPRC-7 – galaxy with non edge-on ring – see Fig. 1) we approximated the ring by the inner-truncated model in order to describe clearly visible hole in the ring component. Fig. 1 shows the results of decomposition for two galaxies with different morphology (edge-on ring, non edge-on ring).

The comparison of our derived apparent magnitudes of PRGs with the SDSS *modelMag* values shows general agreement. Mean differences of the SDSS and our magnitudes are $+0\overset{\rm m}{.}17\pm0\overset{\rm m}{.}31$ (g), $+0\overset{\rm m}{.}10\pm0\overset{\rm m}{.}25$ (r) and $+0\overset{\rm m}{.}09\pm0\overset{\rm m}{.}23$ (i). After excluding 6 most deviated galaxies with magnitudes difference in the g band $\Delta g > +0\overset{\rm m}{.}4$ (SPRC-3, 7, 20, 34, 37, 69), the differences reduce to $+0\overset{\rm m}{.}08\pm0\overset{\rm m}{.}16$ (g), $+0\overset{\rm m}{.}04\pm0\overset{\rm m}{.}14$ (r), and $+0\overset{\rm m}{.}04\pm0\overset{\rm m}{.}16$ (i).

For two galaxies with $\Delta g > +0\overset{\rm m}{.}4$ we have found published results of surface photometry. Brosch et al. (2010) have presented detailed study of SPRC-7 (SDSS J075234.33+292049.8). Our total magnitudes (16.87, 16.42,

Table 1. Basic data for the PRGs sample

Galaxy (1)	Redshift (2)	r (mag) (3)	r_e ($''$) (4)	n (5)	ring/host (6)
SPRC-2	–	14.37	6.9	2.5	0.31
SPRC-3*	0.03683	15.93	2.8	2.1	0.90
SPRC-5	0.02786	17.09	1.5	1.8	0.19
SPRC-6	0.01867	17.02	2.0	1.6	0.11
SPRC-7*	0.06007	16.42	0.9	2.3	1.3
SPRC-9	0.14473	17.47	2.3	1.5	0.36
SPRC-10*	0.04244	16.26	2.9	1.2	0.11
SPRC-11	0.06580	15.67	3.7	3.7	0.11
SPRC-12	0.06247	17.13	1.9	2.2	0.49
SPRC-13	0.03177	15.23	3.1	3.0	0.39
SPRC-14*	0.03188	14.70	4.4	4.5	0.24
SPRC-15	0.03427	14.46	3.3	3.0	0.22
SPRC-16	0.06012	16.98	2.4	1.5	0.32
SPRC-17	0.02640	14.88	7.0	3.2	0.05:
SPRC-18	0.08185	17.40	1.9	1.7	0.15
SPRC-19	0.10516	17.33	1.5	1.9	0.28
SPRC-20	0.07428	16.67	2.6	4.0	0.31
SPRC-23	0.02782	15.94	3.6	1.5	0.25
SPRC-24	0.04710	15.01	3.0	2.6	0.50
SPRC-25	0.07284	17.41	1.5	1.3	0.41
SPRC-27*	0.04835	16.31	2.1	2.4	0.58
SPRC-28	0.07729	16.63	1.5	1.7	0.48
SPRC-29	0.04733	15.49	4.5	2.7	0.16
SPRC-30	0.07517	17.49	1.5	1.0	0.76
SPRC-31	0.04971	15.20	8.5	3.3	0.1:
SPRC-34	0.08131	16.97	–	–	0.37
SPRC-35	0.06757	17.16	1.9	0.8	0.98
SPRC-37	0.06762	16.11	8.3	4.4	0.20
SPRC-39*	0.02933	15.99	4.5	3.1	0.27
SPRC-42	0.02337	15.13	4.0	2.7	1.3
SPRC-44	0.11344	16.55	2.9	1.5	0.20
SPRC-47	0.03123	14.63	8.5	1.9	0.15
SPRC-48	0.05630	15.32	7.9	2.5	0.12
SPRC-49	0.06838	15.91	2.6	1.5	0.05:
SPRC-51	0.07544	17.24	1.0	2.3	0.29
SPRC-53	0.08274	17.63	3.6	0.9	0.36
SPRC-55	0.08581	16.93	1.6	2.3	0.49
SPRC-56	0.05504	14.71	4.9	4.2	0.21
SPRC-57	0.07036	16.39	2.8	1.6	0.51
SPRC-58	–	15.46	2.7	3.4	0.38
SPRC-59	–	16.81	1.5	1.0	0.51
SPRC-63	0.07397	17.58	–	–	0.1:
SPRC-66	0.08738	16.10	2.0	1.7	0.33
SPRC-67*	0.02777	14.07	5.1	3.5	0.46
SPRC-69*	0.02469	15.24	2.1	1.8	0.28
SPRC-70	0.06870	17.59	2.4	0.8	1.3
PRC A-1*	0.01835	14.57	2.6	3.1	0.38
PRC A-4*	0.02341	14.41	6.7	5.1	0.14
PRC A-6*	0.01798	14.76	3.7	2.5	0.49
PRC B-17*	0.00426	13.80	11.9	1.6	0.19

Columns:
(1) name (SPRC or PRC), asterisks mark kinematically-confirmed galaxies,
(2) redshift (SDSS, NED),
(3) total r-band magnitude (present work),
(4) effective radius in the r filter (present work),
(5) Sérsic index in the r band (present work),
(6) ring-to-central galaxy luminosity ratio in the r band (present work).

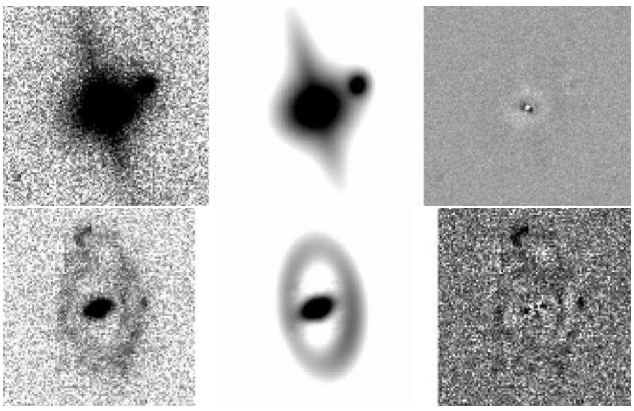

Figure 1. Examples of the PRGs images modeling: SPRC-58 (top), SPRC-7 (bottom). From left to right: original SDSS r-band image, 2D model, residual image.

16.08 in the g, r, i passbands) are in good agreement with Brosch et al. results (16.80, 16.41, 16.12). The parameters of the central galaxy and the ring are in accord also. For the central galaxy Brosch et al. (2010) give such apparent magnitudes: 18.22, 17.35, 16.92 (g, r, i), the same values according to our analysis are 18.28, 17.34, 16.90. The apparent magnitudes of the ring are 17.14, 17.00, 17.01 (Brosch et al. 2010) and 17.21, 17.03, 16.78 (present work). Finkelman et al. (2012) have published photometric data for 16 candidate PRGs, including SPRC-69 from our sample. In the r passband Finkelman et al. give such estimates of apparent magnitudes for SPRC-69: 15.40 (host galaxy), 17.14 (ring), 15.20 (total). Our values are 15.51, 16.90 and 15.24 correspondingly.

In the rest of the paper we will use the results of our photometry for all the sample PRGs (see Table 1 for total magnitudes in the r passband and some other characteristics).

3 RESULTS

3.1 Central (host) galaxies

Fig. 2a-c show distributions of central galaxies by absolute luminosity (corrected for Milky Way absorption according to Schlafly & Finkbeiner 2011 and k-correction from Chilingarian et al. 2010), Sérsic index and physical effective radius. As one can see, they are non-dwarf sub-L^* galaxies with average absolute magnitude $< M_r >= -20.34 \pm 1.04$.

The distribution of Sérsic indices of the host galaxies (Fig. 2b) indicates a broad range of morphologies, from disc-dominated ($n < 1.5$) to bulge-dominated ($n > 3$). It is important to note that n is not a direct measure of the galaxy type and it does not translate one to one to the bulge-to-total ratio. But the single Sérsic index is a reasonable statistical characteristic to separate late-type and early-type galaxies (e.g. Bruce et al. 2012).

The relative fractions of disc-dominated and bulge-dominated brightness distributions are 16%, 28%, respectively, in the r band and 26%, 40% (i filter) in our sample of PRGs hosts. These fractions are consistent with previous findings that late-type galaxies are less frequent among

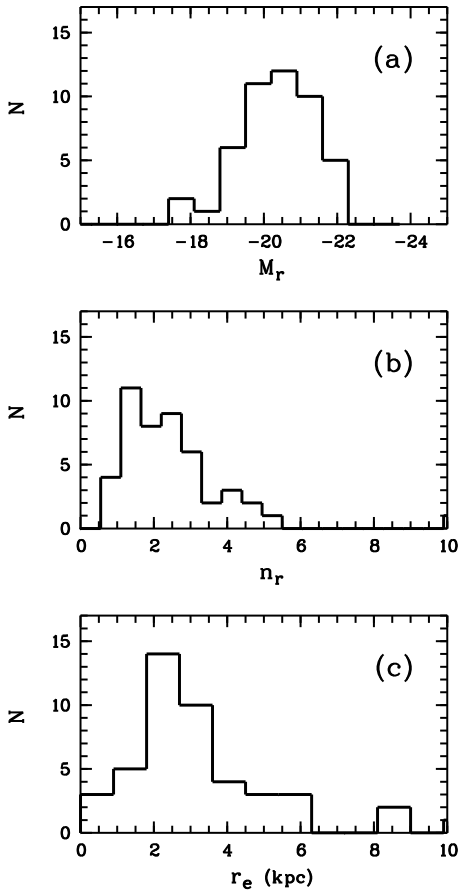

Figure 2. Characteristics of PRGs hosts in the r passband: (a) absolute magnitude, (b) Sérsic index, (c) effective radius.

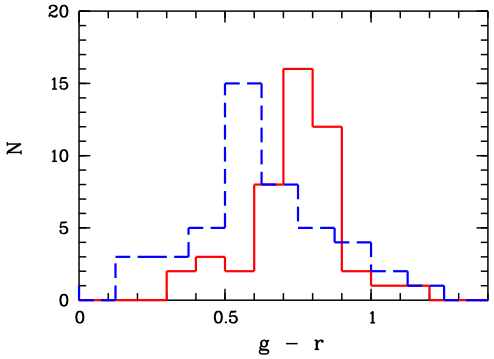

Figure 3. Distribution of the sample galaxies over $g - r$ color of the host galaxies (red solid line) and of the rings (blue dashed line).

PRGs in comparison with ETGs (e.g. Whitmore et al. 1990; Whitmore 1991; Reshetnikov et al. 2011).

Host galaxies of the PRGs show wide distribution of rest-frame optical colors (see the $g-r$ distribution in Fig. 3). In general, the $g - r$ color distribution looks similar to that presented by Finkelman et al. (2012) (see their fig. 6) but the peak in our distribution is shifted to bluer color. (Most probably, this difference can be explained by the absence of k-correction in the Finkelman et al. 2012 data.)

The average colors of the PRGs hosts in our sample are $< g-r >= +0.74 \pm 0.16$, $< r-i >= +0.41 \pm 0.09$. Such colors correspond to the colors of S0 galaxies (Fukugita et al. 2007). Finkelman et al. (2012) have compared the $g-r$ color distribution of PRGs with that of in several control samples of early-type galaxies (normal ETGs, blue ETGs, dusty ETGs). According to fig. 6 in their work, the average color of the PRGs hosts in our sample matches the color of blue early-type galaxies better than typical colors of other types of ETGs. It is important to note that optical colors of PRGs can be distorted by the inner absorption in the hosts and in the rings. Near-infrared photometry of several PRGs was presented earlier by Iodice et al. (2002a,b). They concluded that near-infrared colors of host galaxies are bluer on average than those for standard early-type galaxies.

Fig. 4 shows standard scaling relations for the PRGs hosts. The size – luminosity relation for the hosts is shown in Fig. 4a. PRGs are shifted to lower luminosities in comparison with relation for early type galaxies (at a fixed effective radius) and are located in the same region as spiral galaxies. The characteristics of disc-dominated galaxies in the figure are taken from Simard et al. (2011). Simard et al. (2011) presented results of decomposition for more than 1 million galaxies in the SDSS. We took their decomposition results with pure Sérsic model and selected large ($r_e \geqslant 1.''4$), nearby ($0.01 < z < 0.04$), disc-dominated ($n < 1.5$) galaxies for our Fig. 4.

Fig. 4b demonstrates the Kormendy relation (the mean surface brightness within effective radius r_e vs. r_e in kpc) for PRGs and normal E/S0 galaxies. PRGs follow the standard relation for E/S0 galaxies but, as in Fig. 4a, with notable shift (by $\sim 1^m$) to lower surface brightnesses (at a fixed r_e). This shift is evident for the galaxies with various types of surface brightness distribution ($n < 3$ and $n > 3$). It can be concluded that PRG hosts are more similar to quenched disks than to genuine elliptical galaxies.

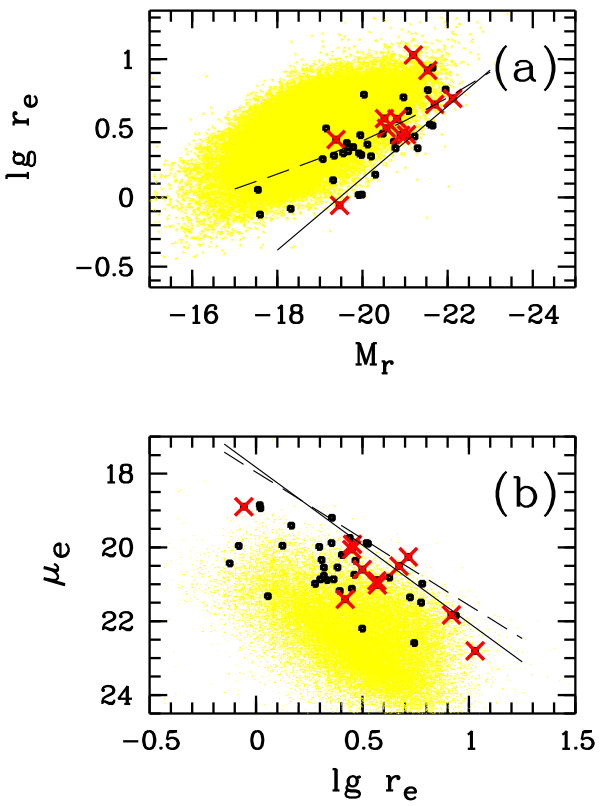

Figure 4. Scaling relations for the host galaxies of PRGs in the r band (dots – galaxies with Sérsic index $n < 3$, red crosses – with $n > 3$): (a) absolute magnitude – effective radius in kpc (solid line gives relation for early type ($n > 2.5$) galaxies, dashed line – for late type with $n < 2.5$, see Shen et al. 2003, yellow dots show the location of $\sim 40\,000$ disc-dominated galaxies from Simard et al. 2011), (b) Kormendy relation (solid line shows the relation for early type galaxies in Coma cluster (Houghton et al. 2012), dashed line represents mean relation for the SDSS early-type galaxies with absolute magnitudes M_r between -18.$^{\rm m}$5 and -22.$^{\rm m}$0 according to Nigoche-Netro et al. 2008, yellow dots are as above).

3.2 Polar structures

Polar structures in our sample of PRGs are, on average, fainter ($< M_r >= -18.90 \pm 1.28$) and bluer ($< g-r >= +0.61 \pm 0.25$, $< r-i >= +0.33 \pm 0.22$) than their host galaxies (Fig. 3; see also Reshetnikov et al. 1994; Iodice et al. 2002b; Finkelman et al. 2012). Taking into account internal extinction in the polar rings (most of them are seen almost edge-on), the difference in colors must be larger. Observed colors of rings are usual for normal spiral galaxies (e.g. Fukugita et al. 2007).

As it was shown earlier by Finkelman et al. (2012), observed luminosities of the hosts and the rings are correlated – more luminous host galaxies possess more luminous rings, on average (Fig. 5). There is also a weak mutual (ring vs. host) correlation of colors but much weaker than in Finkelman et al. (2012). The other possible trend is between the relative size of ring (D_{ring}/D_{host} – diameter of ring normalized by diameter of host galaxy) and absolute magnitude of host galaxy – see Fig. 6. (The rings sizes were taken from Smirnova & Moiseev 2013). Among PRGs with bright central galaxies we see relatively compact rings, while fainter central objects are surrounded by relatively small as far as more extended rings: for bright hosts with $M_r \leqslant -21$ the mean relative size of rings is 1.4±0.4, for faint ones with $M_r \geqslant -20$ the mean value is 2.3±1.2.

We estimated the stellar masses of the rings and the host galaxies following the Bell et al. (2003) approach, which combines a galaxy's luminosity with a mass-to-light ratio from a color measurement. Our calculations employ the $g-r$ colors and r-band luminosities. The results are shown in Fig. 7. As one can see, stellar mass of a polar component is not negligible in comparison with mass of a host in most galaxies. In some galaxies the masses of two components are comparable.

Fig. 8 presents the observed distribution of angle between the ring and the central galaxy. We see that rings in most galaxies are within 20° from polar orientation, so our objects are indeed "polar"-ring galaxies. Relative fraction of such galaxies in the combined sample (our work + Whitmore 1991) is 75% (55 of 73 galaxies). Fig. 8 shows the *projected, apparent* angles between the host galaxy and the ring. Recently, Smirnova & Moiseev (2013) performed analysis of *spatial* angles between two components in the sample

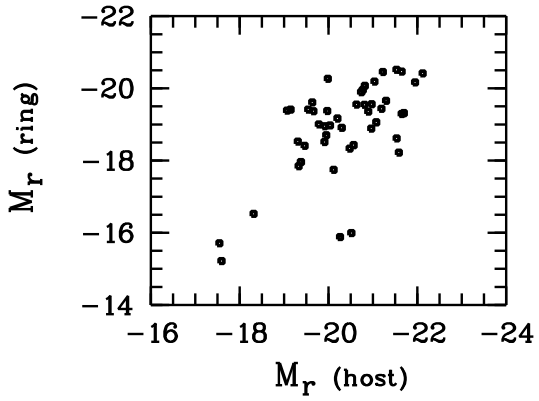

Figure 5. Absolute r-band magnitudes of host galaxies versus rings.

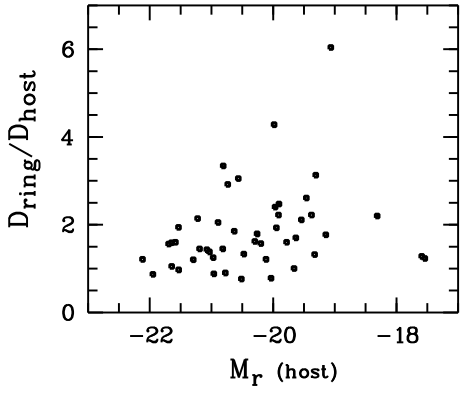

Figure 6. Absolute r-band magnitudes of hosts versus relative sizes of polar rings.

of 78 galaxies from the SPRC and PRC. They came to the same conclusion – in the majority of PRGs the outer structures lie in the plane close to polar within 10°–20°.

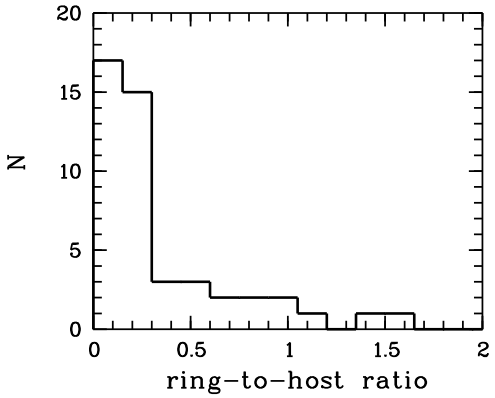

Figure 7. Distribution of the sample galaxies over the ratio of stellar mass of a ring to stellar mass of a host galaxy.

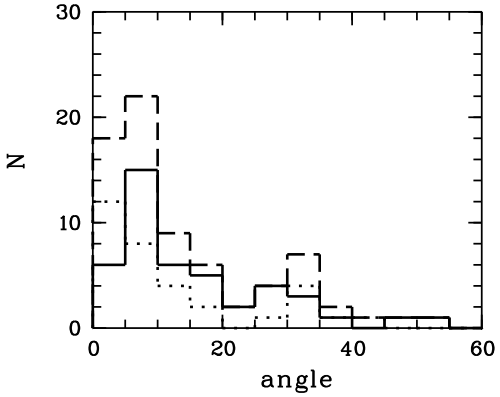

Figure 8. Angular distance away from perpendicularity of the host galaxy and the ring. Solid line – our measurements (g passband), dotted line – the data from Whitmore (1991), dashed line – combined sample.

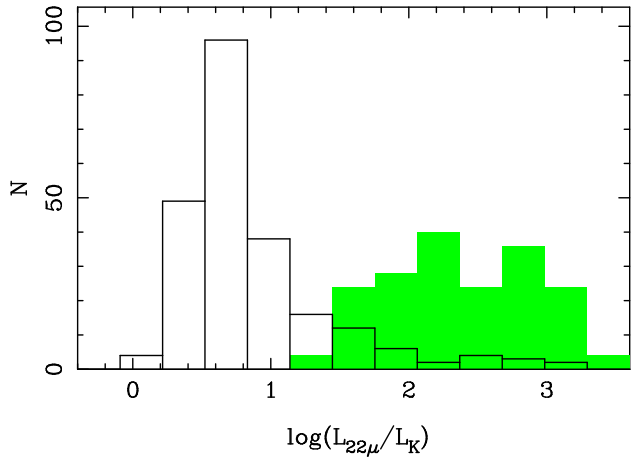

Figure 9. Distribution of our PRG sample galaxies (green) compared to the Atlas^{3D} sample (black line), as a function of the ratio between 22μm and K-band luminosities. The numbers for the PRGs have been multiplied by 4 to compare with the much larger Atlas^{3D} sample.

3.3 Mid-infrared luminosity and star formation rate

All galaxies of our sample were detected in the four bands (3.4, 4.6, 12 and 22μm) of WISE, and we derived the 22μm luminosity in Table 2. From this luminosity, an indication of the star formation rate (SFR) has been derived, following the calibration of Calzetti et al. (2007), also displayed in Table 2. The SFR for PRGs are distributed on the high side of what is found for typical early-type galaxy samples. In Fig. 9, we compare the distribution of the ratio between 22μm and K-band luminosities, with the early-type sample of Atlas^{3D} (Davis et al. 2014). It is clear that the PRG galaxies form relatively more stars than normal early-type galaxies. This shows that the presence of the polar disks, although faint, are significative in this respect.

Also, Fig. 10 shows the distribution of polar rings and hosts in the color-mass diagram. Objects with SFR higher than 2.5 $M_\odot$/yr are plotted with large symbols, PRG rings are clearly in the blue cloud and the hosts are in the yellow

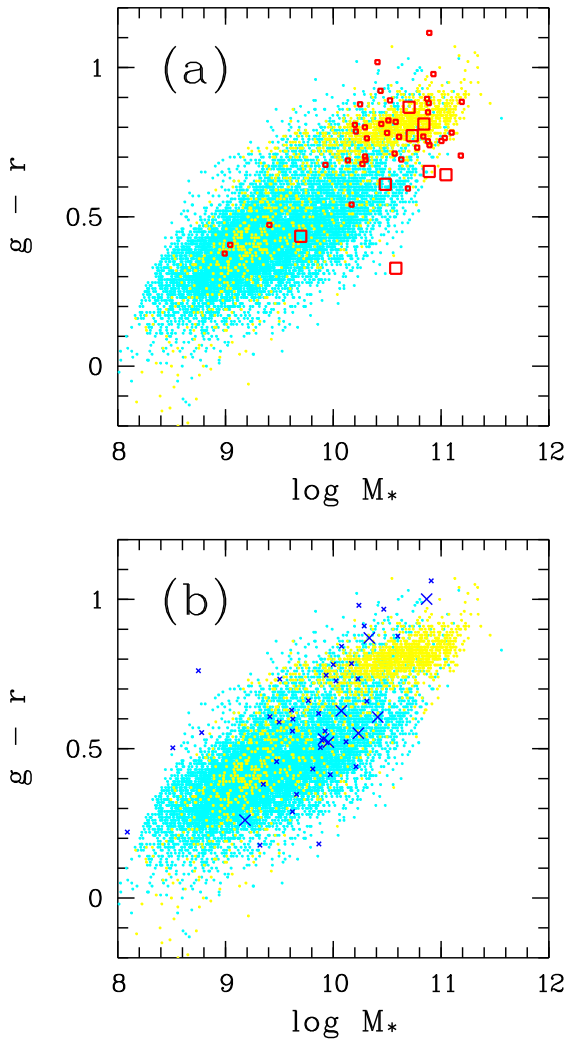

Figure 10. The $g-r$ color – stellar mass (in units of $M_\odot$) diagram (a) of the host galaxies (red symbols) and (b) of the polar rings (dark blue symbols). Galaxies with global star-formation rate >2.5 $M_\odot$/yr are marked by large symbols. Blue and yellow points show locations of nearby ($z = 0.01 - 0.03$) late-type (with Sérsic index n=0.8-1.2) and early-type (n=3.5-4.5) galaxies from Simard et al. (2011) correspondingly. Galaxies with absolute magnitudes $-16 \geqslant M_r \geqslant -23$ are shown only.

one. In Fig. 11, the global colors are plotted in the same diagram (for polar rings and hosts together). The objects at high SFR are distributed in the green valley mainly, showing that this location is due to the symbiose between two different sub-systems.

4 DISCUSSION AND CONCLUSIONS

We have performed a survey of photometric characteristics in a sample of 50 PRGs selected from the SDSS. In general, we have confirmed previous results but on the basis of a much larger and uniform sample.

We have found that central objects of PRGs look like early-type galaxies by morphology and optical colors. Polar structures demonstrate optical colors usual for spiral galax-

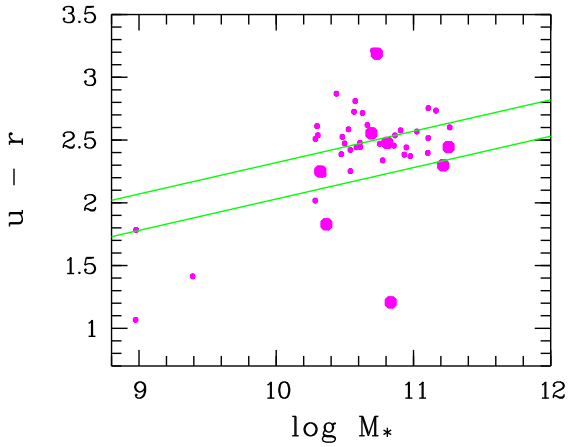

Figure 11. The $u-r$ – mass diagram of the PRGs according to the SDSS total magnitudes corrected for the Milky Way absorption and k-correction. Large symbols show galaxies with star-formation rate >2.5 $M_\odot$/yr, green lines show the green valley (Schawinski et al. 2014).

ies. Typical stellar masses of the rings in our sample are about 10^9–10^{10} $M_\odot$ and they contribute significantly to the total stellar mass of PRGs.

The most interesting results can be seen in Fig. 4. Fig. 4b shows the Kormendy relation for the PRG hosts. It is evident that the location of PRGs is shifted from the relation for E/S0 galaxies. This feature was first noted by Reshetnikov et al. (1994) for bulges of 6 PRGs in the B passband. They discussed this point and proposed that the rings projection distorts the surface brightness distribution of the central regions of galaxies. Projection of an absorbing ring can reduce the observed luminosity of a galaxy and shift its characteristics on the Kormendy relation. Iodice et al. (2002b) found a similar behavior in the K passband for the sample of 5 PRGs. But, since Iodice et al. used observations in the infrared where the dust absorption is minimal, they concluded that this shift can be explained by the small size of the PRG bulges in comparison with normal early-type galaxies. From the other side, our Fig. 4a demonstrates that the PRG hosts are not compact – they are more extended in comparison with E/S0 galaxies of the same luminosities and are located in the locus of spirals. This is true not only of late-type galaxies but also of early-type, bulge-dominated galaxies with $n > 3$. Therefore, an alternative explanation for the shift of the PRGs on the Kormendy relation is that their hosts are fainter (in surface brightness and in luminosity) in comparison with normal early-type galaxies of the same size.

In general, as one can derive from Fig. 4, PRG hosts may represent a transitional class between early- and late-type galaxies. In this sence, they look similar to blue-sequence E/S0 galaxies described by Kannappan et al. (2009). Blue-sequence E/S0 galaxies are shifted from the stellar mass – radius relation for normal ETGs and are located between late-type and early-type galaxies in this plane (see fig. 9 in Kannappan et al. 2009). At a fixed stellar mass, blue-sequence E/S0 galaxies are somewhat larger in size than E/S0 galaxies. This behavior is similar for PRGs: their hosts are larger at a fixed luminosity and they are

Table 2. WISE and 2MASS data for our PRG sample

Galaxy (1)	F_{22} (2)	L_{22} (3)	SFR (4)	L_K (5)
SPRC-3	14.41	42.792	0.94	10.32
SPRC-5	9.13	42.345	0.38	9.36
SPRC-6	6.74	41.859	0.14	9.05
SPRC-7	7.71	42.961	1.33	10.32
SPRC-9	11.58	43.954	10.1	11.28
SPRC-10	10.89	42.797	0.95	10.63
SPRC-11	10.46	43.176	2.06	11.12
SPRC-12	13.51	43.240	2.35	10.27
SPRC-13	8.04	42.406	0.43	10.48
SPRC-14	10.32	42.518	0.54	10.83
SPRC-15	6.42	42.376	0.40	11.02
SPRC-16	11.58	43.138	1.91	10.62
SPRC-17	10.47	42.357	0.39	10.64
SPRC-18	18.05	43.613	5.03	10.59
SPRC-19	10.06	43.592	4.81	10.76
SPRC-20	13.92	43.411	3.33	10.84
SPRC-23	61.94	43.175	2.06	10.64
SPRC-24	12.07	42.935	1.26	11.14
SPRC-25	6.78	43.081	1.70	10.58
SPRC-27	6.99	42.722	0.82	10.53
SPRC-28	6.43	43.112	1.81	10.67
SPRC-29	5.55	42.602	0.64	11.05
SPRC-30	8.23	43.193	2.14	10.54
SPRC-31	13.00	43.016	1.49	10.97
SPRC-34	11.43	43.408	3.31	10.47
SPRC-35	7.39	43.049	1.60	10.38
SPRC-37	10.39	43.198	2.16	11.00
SPRC-39	13.02	42.545	0.57	10.27
SPRC-42	8.25	42.145	0.25	10.39
SPRC-44	8.71	43.600	4.90	11.47
SPRC-47	10.32	42.500	0.52	11.00
SPRC-48	8.08	42.922	1.23	11.13
SPRC-49	8.39	43.116	1.83	11.23
SPRC-51	4.76	42.959	1.33	10.81
SPRC-53	5.79	43.129	1.88	–
SPRC-55	4.97	43.097	1.76	10.82
SPRC-56	4.91	42.685	0.76	11.38
SPRC-57	6.44	43.027	1.52	10.82
SPRC-63	6.61	43.084	1.71	10.55
SPRC-66	117.91	44.488	29.9	11.29
SPRC-67	4.00	41.984	0.18	10.90
SPRC-69	14.93	42.451	0.47	10.43
SPRC-70	13.82	43.336	2.86	10.37
PRCA-1	7.61	41.896	0.15	10.40
PRCA-4	10.86	42.266	0.32	10.67
PRCA-6	5.83	41.763	0.12	10.40
PRCB-17	21.92	41.077	0.03	9.02

Columns:
(1) name (SPRC or PRC),
(2) Flux (22 μm) in mJy,
(3) log Luminosity (22 μm) in erg/s,
(4) SFR in $M_\odot$/yr,
(5) log L_K ($L_\odot$).

located between spirals and ellipticals on the Kormendy relation (Fig. 4a,b).

Kannappan et al. (2009) have noted that blue-sequence E/S0s are often associated with counter-rotating gas and polar rings. We confirmed this conclusion from the opposite point of view – central galaxies of PRGs look similar to blue-sequence E/S0s.

One interesting result is also the distribution of the star formation rate for PRGs. The ratio between 22μm and K-band luminosities is significantly larger for our PRGs sample than for the early-type sample of Atlas^{3D}. PRG galaxies are a symbiotic objects, with two different sub-systems living together, one in the red sequence, the other in the blue cloud, and the global ensemble appears to be in the green valley.

Our results show that the structure of the PRGs hosts are more similar to quenched disks than to ordinary early-type galaxies. More detailed observations and sophisticated modeling required to solve the puzzles of this mysterious class of extragalactic objects.

ACKNOWLEDGMENTS

We thank the referee for useful comments. VR express gratitude for the grant of the Russian Foundation for Basic Researches number 13-02-00416. This work was partly supported by St. Petersburg State University research grants 6.0.160.2010, 6.0.163.2010, and 6.38.71.2012. VR acknowledges the hospitality of Paris Observatory, where a large part of this work was done. FC acknowledges the European Research Council for the Advanced Grant Program Number 267399-Momentum. This publication makes use of data products from the Wide-field Infrared Survey Explorer, which is a joint project of the University of California, Los Angeles, and the Jet Propulsion Laboratory/California Institute of Technology, funded by the National Aeronautics and Space Administration, and data products from the Two Micron All Sky Survey, which is a joint project of the University of Massachusetts and the Infrared Processing and Analysis Center/California Institute of Technology, funded by the National Aeronautics and Space Administration and the National Science Foundation.

REFERENCES

Ahn C., Alexandroff R., Allende P. et al., 2012, ApJS, 203, 21
Bekki K., 1997, ApJ, 490, L37
Bekki K., 1998, ApJ, 499, 635
Bell E.F., McIntosh D.H., Katz N., Weinberg M.D., 2003, ApJS, 149, 289
Bournaud F., Combes F., 2003, A&A, 401, 817
Brook Ch.B., Governato F., Quinn Th., Wadsley J., Brooks A.M., Willman B., Stilp A., Jonsson P., 2008, ApJ, 689, 678
Brosch N., Kniazev A.Y., Moiseev A., Pustilnik S.A., 2010, MNRAS, 401, 2067
Bruce V.A., Dunlop J.S., Cirasuolo M. et al., 2012, MNRAS, 427, 1666
Calzetti D., Kennicutt R.C., Engelbracht C.W. et al., 2007, ApJ, 666, 870
Chilingarian I.V., Melchior A.-L., Zolotukhin I.Yu., 2010, MNRAS, 405, 1409
Combes F., 2014, in E. Iodice & E.M. Corsini eds., Multi-Spin Galaxies, ASP Conference Series, 486, 207
Davis T.A., Young L.M., Crocker A.F. et al., 2014, MNRAS, 444, 3427
Finkelman I., Funes J.G., Brosch N., 2012, MNRAS, 422, 2386

Fukugita M., Nakamura O., Okamura S. et al., 2007, AJ, 134, 579
Houghton R.C.W., Davies R.L., Dalla Bonita E., Masters R., 2012, MNRAS, 423, 256
Iodice E., Arnaboldi M., Sparke L.S., Gallagher J.S., Freeman K.C., 2002, A&A, 391, 103
Iodice E., Arnaboldi M., Sparke L.S., Freeman K.C., 2002, A&A, 391, 117
Kannappan Sh.J., Guie J.M., Baker A.J., 2009, AJ, 138, 579
Maccio A.V., Moore B., Stadel J., 2006, ApJ, 636, L25
Moiseev A.V., Smirnova K.I., Smirnova A.A., Reshetnikov V.P., 2011, MNRAS, 418, 244
Moiseev A., Khoperskov S., Khoperskov A., Smirnova K., Smirnova A., Saburova A., Reshetnikov V., 2014, Baltic Astronomy, in press
Nigoche-Netro A., Ruelas-Mayorga A., Franco-Balderas A., 2008, A&A, 491, 731
Peng Ch.Y.,Ho L.C., Impey Ch.D., Rix H.-W., 2010, AJ, 139, 2097
Reshetnikov V.P., Hagen-Thorn V.A., Yakovleva V.A., 1994, A&A, 290, 693
Reshetnikov V., Sotnikova N., 1997, A&A, 325, 933
Reshetnikov V.P., Faúndez-Abans M., de Oliveira-Abans M., 2011, Astron. Lett., 37, 171
Schawinski K., Urry C.M., Simmons B.D. et al., 2014, MNRAS, 440, 889
Reshetnikov V.P., Faúndez-Abans M., de Oliveira-Abans M., 2011, Astron. Lett., 37, 171
Schlafly E.F., Finkbeiner D.P., 2011, ApJ, 737, id.103
Shen Sh., Mo H.J., White S.D.M. et al., 2003, MNRAS, 343, 978
Simard L., Mendel J.T., Patton D.R., Ellison S.L., McConnachie A.W., 2011, ApJS, 196, 11
Smirnova K.I., Moiseev A.V., 2013, Astrophys. Bull., 68, 371
Whitmore B.C., Lucas R.A., McElroy D.B., Steiman-Cameron T.Y., Sackett P.D., Olling R.P., 1990, AJ, 100, 1489
Whitmore B.C., 1991, in S. Casertano, P.D. Sackett & F.H. Briggs eds., Warped disks and inclined rings around galaxies, Cambridge University Press, 60